Hindawi
Mathematical Problems in Engineering
Volume 2022, Article ID 7582036, 9 pages
https://doi.org/10.1155/2022/7582036

Research Article

Modified High Gain DC-DC Converter with APICs for Microgrid

G. Amritha,[1] G. Kanimozhi,[2] K. Mohana Sundaram,[3] L. Natrayan,[4] and Kiran Ramaswamy[5]

[1]*School of Electrical Engineering, Vellore Institute of Technology, Chennai, Tamil Nadu, India*
[2]*Centre for Smart Grid Technologies, School of Electrical Engineering, Vellore Institute of Technology, Chennai, Tamil Nadu, India*
[3]*Department of Electrical and Electronics Engineering, Centre for Energy Sciences and Engineering, KPR Institute of Engineering and Technology, Arasur, Coimbatore, India*
[4]*Department of Mechanical Engineering, Saveetha School of Engineering, SIMATS, Chennai, Tamil Nadu, India*
[5]*Department of Electrical Engineering, Ambo University, Ambo, Ethiopia*

Correspondence should be addressed to G. Kanimozhi; kanimozhi.g@vit.ac.in, L. Natrayan; natrayan07@gmail.com, and Kiran Ramaswamy; kiran.ramaswamy@ambou.edu.et

Received 8 March 2022; Revised 8 June 2022; Accepted 14 June 2022; Published 5 October 2022

Academic Editor: Ravi Samikannu

This paper proposes a nonisolated high voltage gain DC-DC converter. The active–passive inductor cells (APICs) makes the converter topology expandable, and it also helps in providing a high gain quality at lower duty cycles. The proposed converter is suitable for high gain applications mainly necessitating microgrid as well as integration of renewable energy sources into the existing grid infrastructure. The merits of the converter can be attributed to the ability to achieve high gain and low current stress and switching losses on power electronic switches. The proposed converter is analyzed in both continuous and discontinuous modes of operation, the efficiency is calculated and simulation results substantiate the operation of the converter.

1. Introduction

tIntegration of renewable energy sources into the grid infrastructure and expanding focus on microgrids and their economic as well as environmental significance have compelled a demand for new topologies in converters for high gain applications. This is mainly caused by the low-output voltage derived from these sources, which have always stood as the foremost limitation in their utilization. An extendable converter using APICs is presented [1]. The DC-DC converter introduced is based on the technique that uses three states of switching [2]. The converter is analyzed theoretically and is also verified experimentally through a laboratory prototype. Several other topologies are reviewed to understand their limitations and also to prove the advantages of the proposed topology.

The conventional boost converters do not have the ability to provide high gains owing to the design structure with power switches, diodes, the presence of inductors, and capacitors [3]. The proposed structure is based on parallel charging of inductors during switch ON period and series discharging during switch OFF period. The converter provides high step-up voltage within a shorter range of duty ratio. The converter is based on active switched inductors and passive switched capacitors. Apart from the ability to achieve high gain the topology also achieves high efficiency and reduces voltage stress along with the number of elements in the circuit [4]. The family of transformerless active switched inductor and switched capacitor Cuk converter with high gain ability provides low voltage and current stress. Semiconductor devices with low voltage ratings are used to curtail the conduction losses [5]. Applications like grid-connected PV systems require high step-up voltage. The employment of traditional boost converters in such scenarios are limited. The paper introduces hybrid switched inductor converters to achieve high gain conversion [6].

A hybrid transformerless converter designed with two inductor boost converter consisting of a voltage multiplier and switched capacitor cells is proposed by Andrade et al.

[7]. Improved voltage gain and efficiency, low current and voltage stress, and the ease of operation are some of the key features of the structure. In the two inductor high gain converter topology the difference between two inductor current can be compensated by increasing the inductor current of the corresponding path. This is obtained through increasing the turn-on time. The suggested method has no effect on voltage transfer gain of the converter [8]. Switching structures designed with two capacitors and two-three diodes or two inductors and two-three diodes are described. These can be classified into ldquostep-downrdquo or ldquostep-up.rdquo. These structures when combined with converters such as buck, boost, buck-boost, Cuk, zeta, and sepic converters give a step up function. These converters can increase or decrease the gain more than the classical converters [9].

High gain DC-DC converter integrates voltage RE-Lift, and Super RE-Lift Luo converters have provided sufficient solar energy to the grids. High voltage gain and high power efficiency are benefits of the topology alongside high efficiency. The output voltage is increased in geometric progression. The voltage gain produced by most of the converter structures is narrowed down by the losses [10]. This possesses a limitation in the integration of renewable energy sources using these converters. Melo de Andrade et al. targets series connection of DC-DC converters to prepare an assessment based on Cuk and SEPIC converter topologies [11]. Das and Agarwal studied an expandable high gain converter for microgrid applications. High gain quality is obtained at lower duty cycles themselves. High efficiency, low stress on switches, and minimum output voltage ripple (MOVR) are other benefits [12].

A new series DC-DC converters "XL converters" are suggested by Sayed et al. The main application is renewable energy conversion. The topology is implemented using two buck-boost converters combined with different switched reactive networks [13]. This converter structure offers the feature of high negative voltage at moderate duty ratios. It does not include a transformer and has only a single power control switch. Bidirectional DC-DC converters play a vital role in applications involving increased voltage gain ratios. Asha et al. presented a nonextendable bidirectional buck-boost converter. This topology does not require coupled inductors [14]. The topology has stages of operation and the voltage gain can be derived for n times. Kanimozhi et al. proposed a boost converter based on a new coupled inductor. The structure can be realized for battery charging in photovoltaic systems fed PMDC motor. The closed-loop control is also achieved and maximum possible energy from the PV panels is extorted through the method of single-stage conversion [15].

Improving the output voltage level obtained from various distributed energy sources is very crucial to determine a common voltage throughout the DC link of a particular microgrid. Mahajan et al. intended to eliminate the limitation of the conventional boost converters for this function. The recommended topology provides a quadratic voltage gain. The converter has been validated through comparison with existing topologies and also through loss analysis [16]. The converter proposed by Hossein Hosseini et al. is appropriate for applications involving hybrid electric vehicles. The exceptional aspects include reduction in voltage stress, switching, and conduction losses [17]. The method adopted is that of bipolar switching, to benefit from decreased losses. The converter discussed in Sundaram et al. is nonisolated and maintains a high gain [18]. Low input current ripple makes it a good choice for realizing MPPT in photovoltaic systems. Further assessment of the converter is aided with steady-state analysis, which also justifies the efficacy of the converter.

A DC-DC converter with high gain and without isolation is established on dual coupled inductors by Ahmad et al. achieves high gain via the dual coupled inductors. The topology is consistent with applications involving distributed energy resources. A regenerative snubber circuit is combined to recycle the energy leaked. This converter is promising in transformerless grid-connected PV systems [19]. A magnetically coupled single switch converter implemented by Kanimozhi et al. [20] attains a high voltage ratios on the basis of the inverse operating principle. The applications of the converter are renewable-based energy systems. To prevent core saturation a regenerative circuit is added to the topology [21] that examines a bidirectional DC-DC converter. It consists of coupled inductor and a voltage doubler cell. Extended output voltage is received through a dual active half-bridge circuit. ZVS is utilized for lowering the switching losses. The losses in the semiconductor devices are calculated to compute the losses in the converter. The conduction losses are calculated by multiplying the voltage and current values across individual devices, measured through voltage and current measurement units from the simulation of the converter.

Forouzesh et al. proposed a modular switched capacitor converter topology. The topology is modified from the original Dickson converter. To achieve dynamic variation in gain, two different methods are carried out [22]. The prototype and the equivalent circuits are analyzed with experimental results. The converter design is convenient for green energy-related applications. The structure has been analyzed and the results are presented. Furthermore, the power conversion efficiency has a scope of improvement [23]. A large gain step-up converter is achieved with an asymmetric voltage multiplier network. The converter is designed to mitigate the problem of reverse recovery in the diode of the leakage inductor [24].

2. Proposed Converter

The topology of the proposed converter is depicted in Figure 1. For the analysis, all the inductors are given the same inductance values. The converter is analyzed in both continuous conduction mode (CCM) and discontinuous conduction mode (DCM) of operation.

The circuit diagram of the converter for $n = 1$ is given in Figure 2. The theoretical waveforms for CCM and DCM operation are given in Figure 3. Figure 4 represents the operational modes of the structure and the corresponding circuit diagrams.

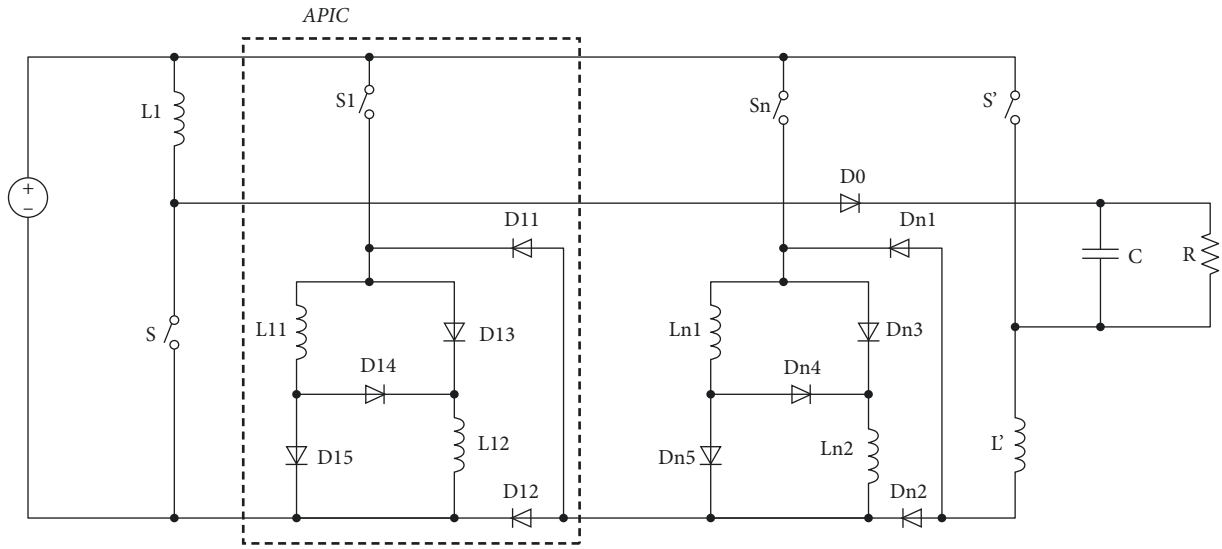

Figure 1: Proposed converter for n APICs.

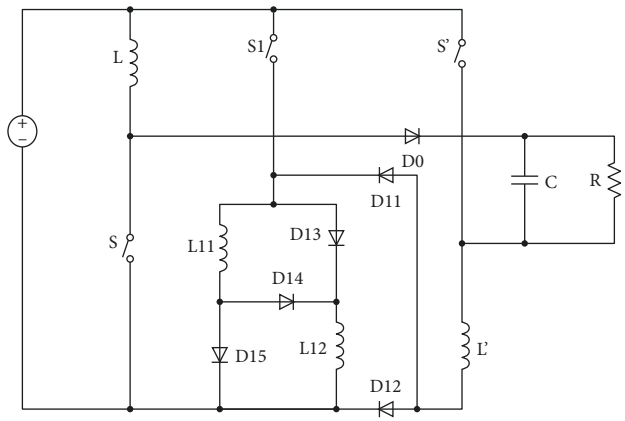

Figure 2: Circuit diagram of the converter for $n = 1$.

3. Analysis of the Converter

3.1. Analysis of the Converter in CCM

3.1.1. Time Interval of T_{ON}. All the switches are turned ON. The voltage across the inductor during this period is given by the following equation:

$$VL = Vi. \tag{1}$$

The inductor current is as follows:

$$i_L = \frac{Vi}{L}t + I_{LV}. \tag{2}$$

In this interval, the inductors get charged therefore the inductor current increases and reaches its maximum value at $t = DT$. Applying $t = DT$ in equation (2) the maximum inductor current can be derived as follows:

$$ILP = \frac{ViDT}{L} + I_{LV}. \tag{3}$$

The capacitor is discharged by the interval end, and the capacitor voltage decreases to V_{CV}.

3.1.2. Time Interval of T_{OFF}. All the switches are OFF. The voltage across the inductor can be given as follows:

$$VL = \frac{Vi - Vo}{2n + 2}. \tag{4}$$

n is the number of APICs. For this interval the current across the inductors is as follows:

$$i_L = \frac{Vi - Vo}{(2n + 2)L}t + I_{LP}. \tag{5}$$

At the end of this interval, the inductor current will be equal to I_{LV}, since the current decreases as a result of the inductor discharging. Applying $t = (1 - D)T$ in equation (4), the minimum inductor current is as follows:

$$i_L = \frac{(Vi - Vo)(1 - D)T}{(2n + 2)L} + I_{LP}. \tag{6}$$

As the current across inductors and the capacitor decreases at this interval, inductor provides the load current along with charging the capacitor.

3.1.3. Voltage Gain Calculation. Considering equations (1) and (3), the voltage gain can be derived as follows:

$$\frac{Vo}{Vi} = \frac{1 + D(2n + 1)}{(1 - D)}. \tag{7}$$

The converter is designed considering minimum output voltage ripple. Least OVR is obtained in CCM operation. The value of the inductor is calculated as given in Table 1. The voltage gain as well as the output ripple of the converter is independent of the inductance value.

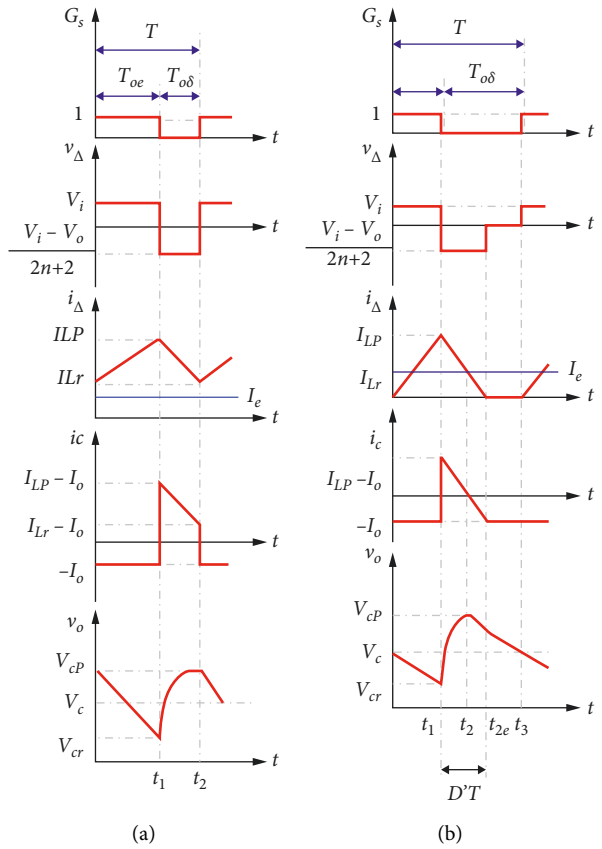

Figure 3: Theoretical waveforms. (a) CCM. (b) DCM.

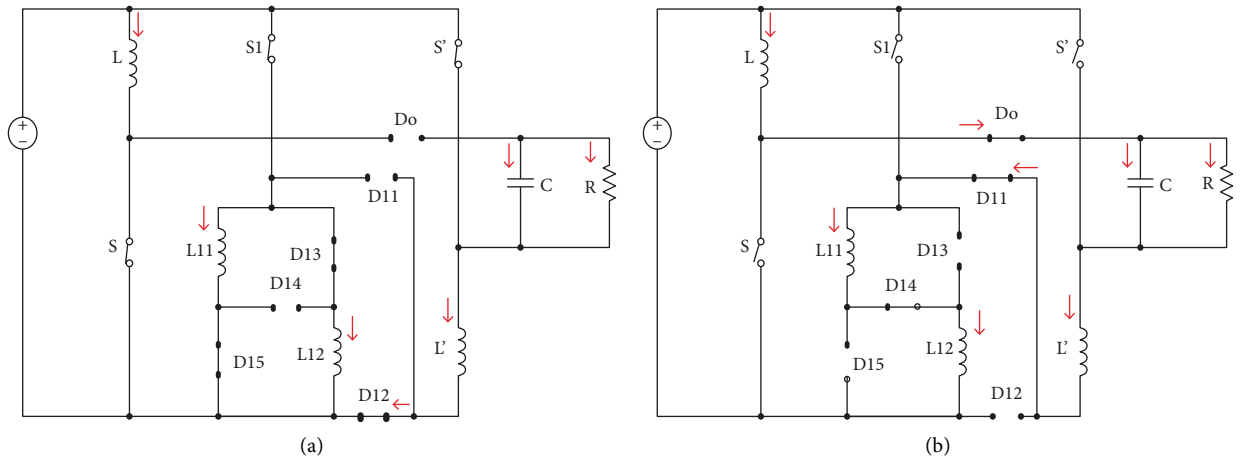

Figure 4: Operation modes diagram of the converter for $n = 1$. (a) T_{ON}. (b) T_{OFF}.

Table 1: Different operational modes in the converter versus inductance values.

Inductance values	Operational mode
$L > L_C$	CCM
$L < L_C$	DCM

3.1.4. Voltage Stress and Current Stress. The voltage stress across the switches and the diodes depends upon the voltage gain and the number of APICs and can be formulated as a function of the same. Since the ripple factor of the converter is considerably low (~2%), the voltage and current stress of the converter are reduced.

Table 2: Simulation parameters.

Simulation parameter	Value
Output voltage, (V_0)	400 V
Switching frequency, (F)	50 kHz
Load resistance, (R)	50–100 Ω
Capacitance, (C)	200 mF
Output power, (P_0)	2 kW
Input voltage (V_i)	20 V–40 V
Inductance, (L_c)	11.3 μH

3.2. Analysis of the Converter in DCM

3.2.1. Time Interval of T_{ON}. At this time interval, the analysis is the same as that of CCM, therefore the maximum current through the inductor is given as follows:

$$i_{LP} = \frac{Vi\ DT}{L}. \tag{8}$$

3.2.2. Time Interval of T_{OFF}. At this time interval, the capacitor current equals the load current. The capacitor voltage decreases as the capacitor discharges. The maximum inductor current is as follows:

$$I_{LP} = \frac{(Vo - Vi)DT}{(2n+2)L}. \tag{9}$$

3.3. Critical Inductance. The minimum inductor current is given as follows:

$$I_{LV} = Io\left(\frac{1}{1-D} - \frac{R\ D}{2Lf}\frac{(1-D)}{[1+(2n+1)D]}\right). \tag{10}$$

Applying $I_{LV} = 0$ (10), the critical inductance between CCM and DCM can be obtained as follows:

$$L_c = \frac{R\ D(1-D)}{2f}\frac{Vi}{Vo}. \tag{11}$$

4. Design Considerations

The converter components are designed to obtain suitable operation with less output voltage ripple. The critical inductance is derived as a function of V_i and R. For a particular value of inductance the converter can operate in either CCM or DCM mode, as given in Table 1. The output voltage of the converter is less in CCM operation than that of DCM [25]. The converter is specified for renewable energy integration with the grid in microgrids. In these cases the quality of the waveform is crucial. Therefore maintaining MOVR is a very important condition considering these aspects. The converter is suitable for such applications.

5. Simulation Results

The simulation results are discussed to validate the converter topology. The converter parameters are verified for $n = 1$. The converter parameters are consolidated in Table 2. The critical inductance value obtained is $L_C = 11.3\,\mu$H. The simulation is implemented in both modes of operation. The CCM analysis is performed for $L = 20\,\mu$H and DCM analysis is performed for $L = 5\,\mu$H. Figures 5 and 6 show the output waveforms attained for CCM. The output waveforms obtained for DCM are presented in Figures 7 and 8. It can be inferred from the waveforms that voltage stress is highest in the diode at the output side. An output voltage ripple (OVR) of 2% is produced. The MOVR does not depend upon inductance value.

For further analysis, the theoretical and simulation results are compared. The efficiency as well as the voltage gain of the topology are improved with the increase in n (number of APICs). The efficiency reduces with an increase in the number of passive elements.

The capacitive filter of the converter is calculated based on minimum output voltage ripple. The ripple factor is considered to be 2% and the C value is calculated from the following equation:

$$C = \frac{D}{\mathrm{Rrf}}. \tag{12}$$

where C is the capacitance in farad, R is resistance, r is the ripple factor, and f is the switching frequency.

6. Comparison

A conventional boost converter and an extendable high gain converter is used for comparing the topology. The comparison among different parameters of the same is given in Table 3. The output voltage and the corresponding voltage gain increases with an increase in 'n' APICs. This converter is appropriate for application in microgrids for integrating renewable energy systems into the grid. Reasonably high values of voltage gain can be obtained at lower values of duty ratios. The number of inductors and passive elements in the topology is lesser than other extendable topologies. Considering the overall losses contributed by the semiconductor devices, major proportion (approximately 98%) is contributed by the total diodes used in the design. But with respect to the topology used for comparison, the losses are further reduced since the number of diodes in the design are less by a number of 5 and the inductors by a number of 2. Therefore the losses are reduced. Small inductance values are sufficient.

All the inductors in the topology are considered to be of the same value to make the analysis of the converter simpler. Voltage gain of the converter depends upon the number of

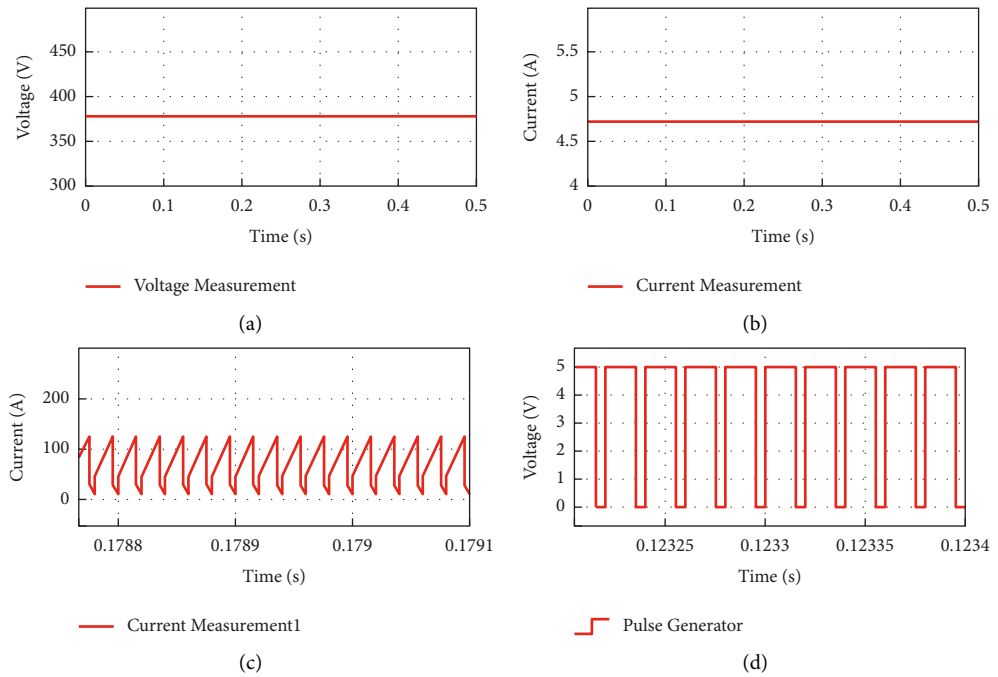

Figure 5: Simulation results in CCM. (a) Output voltage. (b) Output current. (c) Inductor current. (d) Switching pulse.

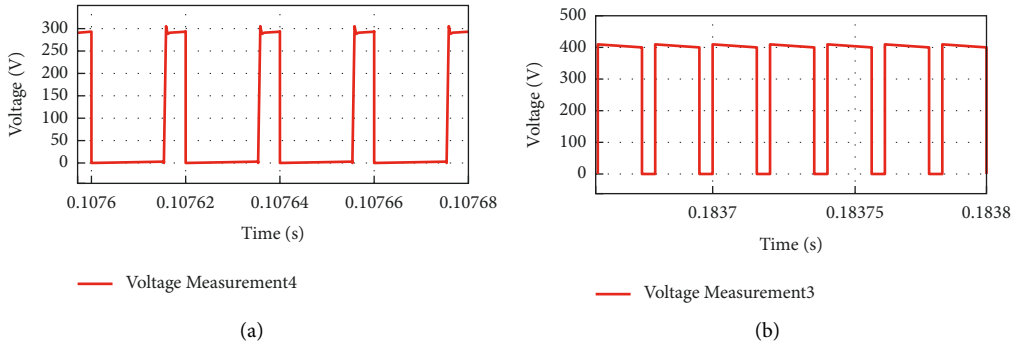

Figure 6: (a) Voltage stress across switches S' in CCM. (b) Voltage stress across diode Do in CCM.

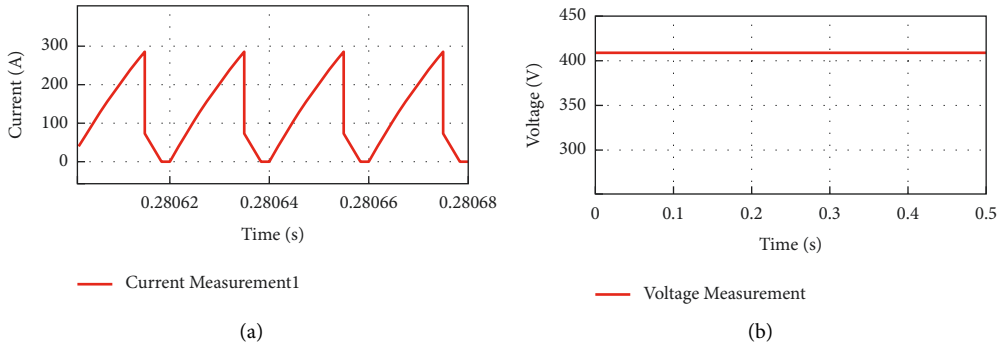

Figure 7: Continued.

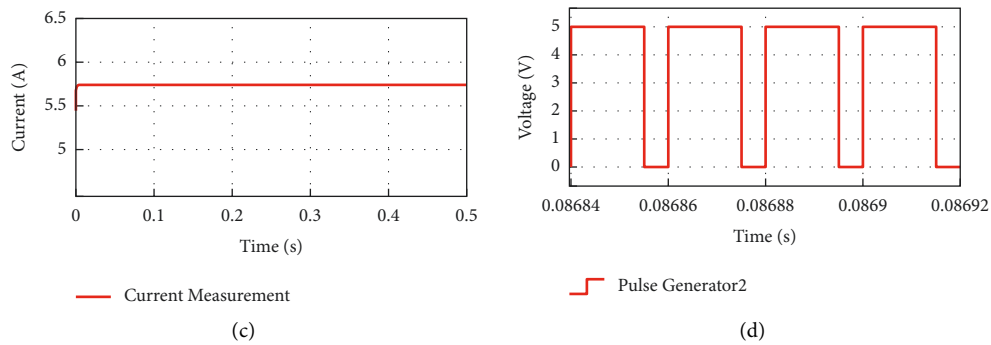

Figure 7: Simulation results in DCM. (a) Output voltage. (b) Output current. (c) Inductor current. (d) Switching pulse.

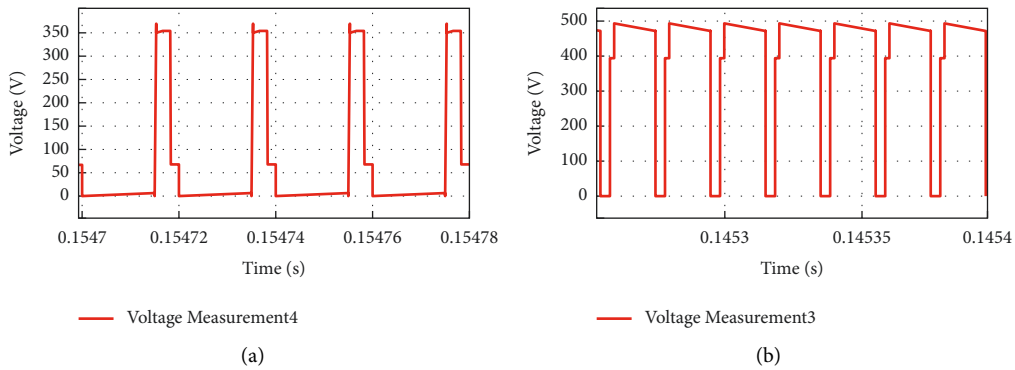

Figure 8: (a) Voltage stress across switches S' in DCM. (b) Voltage stress across diode Do in DCM.

Table 3: Results comparison.

Elements	Boost converter	Extendable nonisolated converter	Proposed converter
Diodes	1	$5n+6$	$5n+1$
Switches	1	$n+2$	$n+2$
Inductors	1	$2n+4$	$2n+2$
Voltage gain	$1/1-D$	$1+(2n+3)D/1-D$	$1+(2n+1)D/1-D$
Efficiency	98.33%	95.6%	96.6%

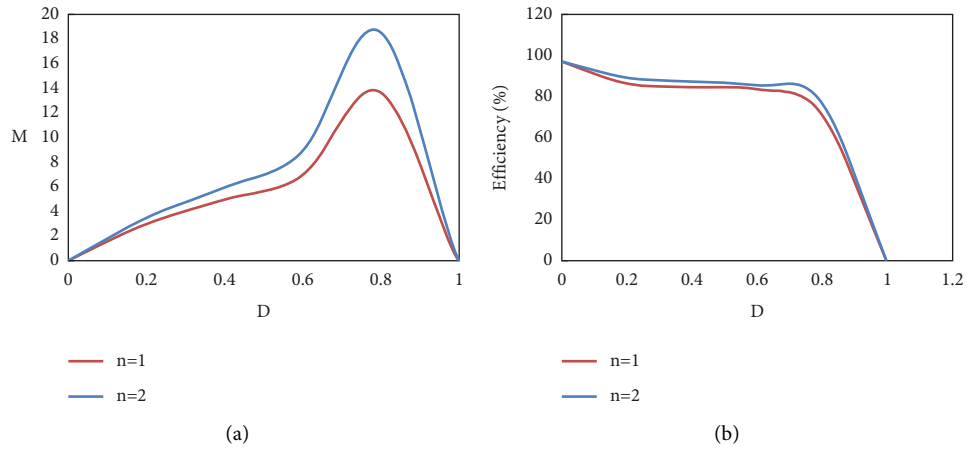

Figure 9: (a) Voltage gain versus duty cycle. (b) Efficiency versus duty cycle.

inductors in the circuit, which is derived assuming same inductors. If the inductors of different inductance values are considered, then analysis of the converter will be different. But even in such cases the final result of the main parameters will be similar. The proposed converter efficiency all though higher than the topology used for comparison is less than that of the conventional boost converter. However the comparison of efficiency is not approved due to certain factors of consideration. Furthermore, the variation in voltage gain and the efficiency with respect to duty cycle that are plotted and compared for $n = 1$ and $n = 2$ are shown in Figure 9. From the plot of efficiency versus duty cycle it can be validated that for a typical value of duty cycle the efficiency of the converter is improved with the increase in n.

7. Conclusion

An extendable high gain DC-DC converter has been proposed for microgrid applications. Since the topology involves active–passive inductor cells the topology can be extended to provide improved voltage gain. The voltage stress on semiconductor devices is low, thereby reducing the losses. The inductors required are of small size. The proposed topology can achieve high gains at lower values of the duty cycle, which is difficult to accomplish from conventional boost converters. The topology is compared with conferred literature structures and the conventional boost converter. The converter elements are designed based on MOVR. The simulation results validate the merits of the proposed converter.

Data Availability

The data used to support the findings of this study are included in the article. However, the reader may contact the corresponding author for more details on the data.

Conflicts of Interest

The authors declare that there are no conflicts of interest regarding the publication of this paper.

Acknowledgments

The authors thank Vellore Institute of Technology, Chennai, for the technical assistance. The authors appreciate the supports from Ambo University, Ethiopia.

References

[1] E. Babaei, H. Mashinchi, M. Sabahi, and S. H. Hosseini, "Extendable non-isolated high gain DC-DC converter based on active- passive inductor cells," *IEEE Transactions on Industrial Electronics*, vol. 65, no. 12, pp. 9478–9487, 2018.

[2] F. L. Tofoli, D. de Souza Oliveira, R. P. Torrico-Bascopé, and Y. J. A. Alcazar, "Novel nonisolated high-voltage gain DC–DC converters based on 3SSC and VMC," *IEEE Transactions on Power Electronics*, vol. 27, no. 9, pp. 3897–3907, 2012) Novel.

[3] Y. Sheng, T. Juu, and J. F. Chen, "Lung "Transformerless dc-dc converters with high step-up voltage gain," *IEEE Transactions on Industrial Electronics*, vol. 56, no. 8, pp. 3144–3152, 2009.

[4] M. A. Salvador, J. M. de Andrade, T. B. Lazzarin, and R. F. Coelho, "Nonisolated high-step-up dc-dc converter derived from switched-inductors and switched-capacitors," *IEEE Transactions on Industrial Electronics*, vol. 67, no. 10, pp. 8506–8516, 2020.

[5] A. M. S. S. Andrade, T. M. K. Faistel, A. Toebe, and R. A Guisso, "Family of transformerless active switched inductor and switched capacitor cuk DC–DC converter for high voltage gain applications," *IEEE Journal of Emerging and Selected Topics in Industrial Electronics*, vol. 2, no. 4, pp. 390–398, 2021.

[6] yu Tang, D. Fu, T. Wang, and Z. Xu, "Hybrid switched-inductor converters for high step-up conversion," *IEEE Transactions on Industrial Electronics*, vol. 62, no. 3, pp. 1480–1490, 2015.

[7] A. Andrade, T. Faistel, R. Guisso, and A. Toebe, "Hybrid high voltage gain transformerless DC–DC converter," *IEEE Transactions on Industrial Electronics*, vol. 69, no. 3, pp. 2470–2479.

[8] Z. Y. Chen, Z. D. Lu, Y. Chen, and Y. Wu, "Two-inductor high-voltage-gain converter with turn-off delay controlled current-sharing method," *Electronics Letters*, vol. 56, pp. 508–510, 2020.

[9] B. Axelrod, Y. Berkovich, and A Ioinovici, "Switched-capacitor/switched-inductor structures for getting transformerless hybrid DC–DC PWM converters," *IEEE Transactions on Circuits and Systems I: Regular Papers*, vol. 55, no. 2, pp. 687–696, 2008.

[10] H. Gholizadeh, S. Aboufazeli, Z. Rafiee, E. Afjei, and M. Hamzeh, "A Non-isolated High Gain DC-DC Converters with Positive Output Voltage and Reduced Current Stresses," in *Proceedings of the 11th Power Electronics, Drive Systems, and Technologies Conference (PEDSTC)*, Tehran, Iran, February 2020.

[11] J. Melo de Andrade, M. A. Salvador, R. F. Coelho, and T. B. Lazzarin, "General method for synthesizing high gain step-up DC–DC converters based on differential connections," in *Proceedings of the IEEE Transactions on Power Electronics*, vol. 35, no. 12, December 2020.

[12] M. Das and V. Agarwal, "Generalized Small Signal Modeling of Coupled-Inductor-Based High-Gain High-Efficiency DC–DC Converters," in *Proceedings of the IEEE Transactions on Industry Applications*, June 2017.

[13] S. S. Sayed, ElM. Mena, M. Elmenshawy, L. Ben-Brahim, and M. Ahmed, "Design and Analysis of High-Gain Medium-Voltage DC-DC Converters for High-Power PV Applications," in *Proceedings of the 2018 IEEE 12th International Conference on Compatibility, Power Electronics and Power Engineering (CPE-POWERENG 2018)*.

[14] P. Asha, L. Natrayan, B. T. Geetha et al., "IoT enabled environmental toxicology for air pollution monitoring using AI techniques," *Environmental research*, vol. 205, Article ID 112574, 2022.

[15] G. Kanimozhi, O. V. Gnana Swathika, K. Logavani, and A. Ambikapathy, "High gain DC-DC converter with extendable APIC's," *Materials Today Proceedings*, 2020.

[16] S. Mahajan, S. Padmanaban, and J. K. Pedersen, "Jens Bo Holm-Nielsen, Zbigniew Leonowicz," XL Converters- New Series of High Gain DC-DC Converters for Renewable Energy Conversion"" in *Proceedings of the IEEE International Conference on Environment and Electrical Engineering*, Genova, Italy, June 2019.

[17] S. Hossein Hosseini, R. Ghazi, S. Farzamkia, and M. Bahari, "A Novel High Gain Extendable DC-DC Bidirectional Boost-

Buck Converter," in *Proceedings of the 11th Power Electronics, Drive Systems, and Technologies Conference*, Tehran, Iran, February 2020.

[18] M. SundaramK, P. Prakash, S. Angalaeswari, T. Deepa, L. Natrayan, and P. Paramasivam, "Influence of process parameter on carbon nanotube field effect transistor using response surface methodology," *Journal of Nanomaterials*, vol. 2021, p. 1, 2021 7739359.

[19] J. Ahmad, M. Zaid, A. Sarwar et al., "A new high-gain DC-DC converter with continuous input current for DC microgrid applications," *Energies*, vol. 14, no. 9, p. 2629.

[20] G. Kanimozhi, C. Umayal, and S. Dhanasekar, "FPGA based Hybrid Resonant Switching DC/DC converter for Electric Vehicles," *International Journal of Innovative Technology and Exploring Engineering (IJITEE) ISSN: 2278-3075*, vol. 89 pages, July 2019.

[21] H. Ardi, A. Ajami, and M. Sabahi, "A novel high step-up dc-dc converter with continuous input current integrating coupled inductor for renewable energy applications," *IEEE Transactions on Industrial Electronics*, In press, 2017.

[22] M. Forouzesh, Y. Shen, K. Yari, Y. P. Siwakoti, and F. Blaabjerg, "High-efficiency high step-up dc-dc converter with dual coupled inductors for grid-connected photovoltaic Systems," *IEEE Transactions on Industrial Electronics*, In press, 2017.

[23] Y. P. Siwkoti, F. Blaabjerg, and P. C. Loh, "High step-up trans inverse dc-dc converter for the distributed generation system," *IEEE Transactions on Industrial Electronics*, vol. 63, no. 7, pp. 316–322, 2016.

[24] H. Wu, K. Sun, L. Chen, L. Zhu, and Y. Xing, "High step-up/stepdown soft-switching bidirectional dc-dc converter with coupled inductor and voltage matching control for energy storage systems," *IEEE Transactions on Industrial Electronics*, vol. 63, no. 5, pp. 2892–2903.

[25] D. K. Jain, S. K. S. Tyagi, S. Neelakandan, M. Prakash, and L. Natrayan, "Metaheuristic optimization-based resource allocation technique for cybertwin-driven 6G on IoE environment," *IEEE Transactions on Industrial Informatics*, vol. 18, no. 7, pp. 4884–4892, 2022.